Published in final edited form as:
Chemistry. 2010 September 17; 16(35): 10616–10628. doi:10.1002/chem.201001018.

Kinetic Isotope Effects in Asymmetric Reactions

Thomas Giagou[a] and **Matthew P. Meyer**[a,*]

[a]School of Natural Sciences, University of California Merced, 5200 N. Lake Rd., Merced, CA 95344 (USA)

Abstract

Kinetic isotope effects are exquisitely sensitive probes of transition structure. As such, kinetic isotope effects offer a uniquely useful probe for the symmetry-breaking process that is inherent to stereoselective reactions. In this Concept article, we explore the role of steric and electronic effects in stereocontrol, and we relate these concepts to recent studies carried out in our laboratory. We also explore the way in which kinetic isotope effects serve as useful points of contact with computational models of transition structures. Finally, we discuss future opportunities for kinetic isotope effects to play a role in asymmetric catalyst development.

Keywords

asymmetric reactions; kinetic isotope effects; reaction mechanisms; stereoselection; steric hindrance

Introduction

The development of new stereoselective reactions is an extremely active area of research. Surprisingly, few mechanistic methods have been designed to probe the mechanistic features that are unique to stereoselective reactions. Of particular interest are the physical interactions that serve to break symmetry in proceeding from the reactant to the transition state on the reaction coordinate. A simple view from which to approach this problem is that stereoselection is mediated by a compromise between favorable orbital overlap and steric repulsion in the transition state. With that view in mind, we require a tool that is capable of measuring how the forces around atoms of interest change as a reactant traverses the reaction coordinate. Kinetic isotope effects (KIEs) yield precisely this information.

KIEs are capable of elucidating reaction mechanisms at a number of different levels of detail. At the simplest level, KIEs can serve to identify the rate-limiting step in a mechanism or eliminate or corroborate candidate mechanisms.[1] At a more detailed level, KIEs can be used to understand changes in bonding and environment that occur at the transition state, including discrete changes in bond order, hyper-conjugation, and steric repulsion.[2] Computational transition-structure models that employ density functional theory have been enormously successful in computing KIEs that are in excellent accordance with experimentally determined values.[3] These models serve as a tool by which the physical origins of KIEs in stereoselective reactions can be further explored.

Fax :(+1)209-228-4646 mmeyer@ucmerced.edu.

To probe the symmetry-breaking process inherent to the enantioselective reactions described below, an essential design feature is required. Enantiotopic groups are employed within the reactant. At the transition state, these groups become diastereotopic, and, as a consequence, experience distinct environments (Scheme 1). Enantiotopic groups that reside close to the nascent stereogenic center can be used to understand how transition structure translates into stereocontrol. Because KIEs are typically very sensitive to transition structure, these measurements can be used to understand electronic, steric, and other effects. Results from these experiments have led us to try to better understand the physical signatures of nonbonding interactions. This Concept summarizes our efforts over the past three years to develop methods for mechanistic inquiry into asymmetric reaction mechanisms and to understand the physical determinants of stereoselection.

How KIEs Inform Mechanism

KIEs measure the extent to which changes in isotopic identity at a given position in a reactant molecule affect the rate.[4] Not surprisingly, the effects of isotopic substitution at positions where bonds are broken or formed can be sizable. In fact one of the most frequent applications of KIEs has been as a tool for the corroboration or rejection of mechanistic schemes. Isotope effects that occur where bonds are broken or formed are known as primary KIEs. In addition to aiding in the identification of rate-determining steps and helping to create and refine mechanistic schemes, primary KIEs have been indispensible tools in understanding tunneling[5,6] and dynamical phenomena.[3f,g, 7]

Primary (1°) KIEs occur at sites where bonding changes (i.e., bond breakage or formation) occur. A simple model for the origin of 1° KIEs is shown in Figure 1. In this simple model, an example utilizing the stoichiometric DIP-Cl reduction is provided. The isotope effect arises because of the difference in zero-point energies in the reactant C–H(D) stretches for the positions denoted in bold text. As the reactant proceeds along the reaction coordinate, a point is reached at which the transferred hydride(deuteride) has no restoring force, thus making the frequency corresponding to its motion imaginary. This defines the unstable vibrational mode at the transition state. Because this mode has no zero-point energy, the difference in the free energies of reaction arise from the differences in zero-point energy within the C–H(D) bonds in the reactant, DIP-Cl. This difference causes protiated DIP-Cl reductant to react at a greater rate than [D_2]DIP-Cl reacts. This model is only a first-order approximation, but it explains why primary KIEs are normal (i.e., $k_{light}/k_{heavy} > 1$). A model that refines this view by taking into account transverse vibrations that compensate zero-point energy in the transition state has been developed by Westheimer.[8] The effect of compensatory zero-point energy contributions in the transition state is an overall attenuation in the observed primary KIE. An additional effect, tunneling, has been shown to significantly amplify primary KIEs over what would be expected from simple zero-point energy effects. Primary KIEs are also frequently observed at heavy atom (C, N, O, Cl) positions and are helpful in identifying the rate-limiting step in a reaction.[9]

Secondary (2°) KIEs are typically more subtle than primary KIEs; however, they can be more useful in developing cogent models of transition structure. This is largely because they can typically originate in a number of positions and can reflect changes in vibrational force constants arising from a number of physical phenomena. Although it is something of an oversimplification, the origin of secondary KIEs will be explained as if the vibrational modes being affected by isotope substitution are orthogonal to the reaction coordinate. Figure 2 illustrates the concept of a 2°-^{2}H KIE arising from steric repulsion developing in the DIP-Cl reduction transition state. The force constants describing C–H stretching modes become tighter in the indicated pro-*S* position. This results in a greater increase in zero-point energy for isotopologues possessing the CH_3 (versus CD_3) group in proceeding from

reactants to the transition state. This effectively makes the free energy of activation higher for the protiated isotopologue, resulting in an inverse (i.e., $k_{light}/k_{heavy}<1$) ^{2}H KIE. A metaphor for this situation is the sumo match illustrated in the frontispiece. In fact, ^{2}H KIEs resulting from steric interactions are inverse, as would be expected from this simple model.[10] Of course, secondary KIEs can also be normal (i.e., $k_{light}/k_{heavy}>1$). A metaphor for normal KIEs is the foot race illustrated in the frontispiece. Normal secondary ^{2}H KIEs typically arise from situations in which C–H(D) bonds donate hyperconjugatively into unfilled orbitals,[11] or there is a decrease of p character at an atom bearing the isotopically substitution (i.e., $sp^3 \rightarrow sp^2$ or $sp^2 \rightarrow sp$),[12] or in conversions of olefinic positions to radical-bearing centers.[13] In the first case listed above, it is the C–H(D) stretching frequencies that are most affected. In the cases of hybridization change or the development of a radical center, it is out-of-plane vibrations and torsional motions, respectively, that have reduced force constants in the transition state.

The research described herein seeks to utilize both experiment and theory in concert to elucidate the origins of stereoselection. KIE measurements are nothing more than relative rate measurements. As such, KIEs are determined entirely by differences in the free energies of activation for the isotopologues or isotopomers being compared. The transition state is really an ensemble frequently composed of conformationally similar structures. Calculations of KIEs often make the assumption that the transition state can be reasonably well represented by the appropriate first order saddle point upon the potential energy surface. By and large, this approximation works well in most cases and has been demonstrated to be widely applicable. Situations can arise, however, when this approximation is a poor one. In some cases variational effects due to zero-point energy differences among isotopologues can alter the effective dividing surface that separates reactants and products such that the first-order saddle point is somewhat distant from the dividing surface.[14,15] Furthermore, the dividing surface can strongly depend upon isotopic substitution. Another difficult class of cases is those for which no first-order saddle point exists in the trajectory from reactant(s) to product(s). In these “barrierless” reactions, the free energy of activation is completely entropic.[16] Another potential complication is solvent friction, which can give rise to isotope-dependent transition-state recrossing.[17,18] This effect is likely to be especially problematic in systems in which proton or hydride transfer occurs. Finally, dynamic corner cutting has been identified in a few gas-phase systems. This phenomenon results from conformational sampling due to excess (or even zero point) vibrational energy residing in the reactant that allows the traversal of the dividing surface between reactants and products at a point distant from the first-order saddle point.[19,20] In spite of the potential complications arising from the use of transition structures or first-order saddle points to describe the transition state, it appears to be a robust approximation in most cases.

Steric Repulsion and Stereoselection

One of the most evident guiding principles in predictive models of stereoselection is that the major stereochemical pathway proceeds through a transition state in which steric repulsion is minimized. This design feature is illustrated very clearly for aldol reactions that utilize *Z*-boron enolates as nucleophiles[21] (Scheme 2A) and Claisen rearrangements[22] (Scheme 2B). In these models, the avoidance of repulsive 1,3-diaxial interactions in a chairlike transition state and eclipse strain resulting from boatlike transition states, respectively, determines the major stereochemical pathway. In addition to the two particularly clear examples mentioned above, there are numerous specific and general models that employ the avoidance of steric repulsion as a guiding principle.[23–30] While it is widely accepted that the avoidance of unfavorable steric interactions is a key determinant of stereoselection, it is not clear how closely balanced steric repulsion and various orbital overlap interactions are. Such considerations are essential to understanding the degree to which electronically

favorable arrangements of atoms can be perturbed by steric interactions without sacrificing stereocontrol.

Steric Repulsion and KIEs

Each of the models for predicting stereochemistry mentioned above incorporates the avoidance of significant steric repulsion as a fundamental design feature.[23–30] Deuterium KIEs offer a direct method for probing steric repulsion. Steric ^{2}H KIEs originate from quantum mechanical differences in the vibrational wavefunctions of C–H and C–D bonds. Considering the quantum nature of C–H(D) bonds, C–D bonds are effectively shorter than C–H bonds for two reasons (Figure 3): The first cause of disparity in C–H and C–D bond lengths arises because of the anharmonic nature of the vibrational wells that describe C–H stretching modes. Because the zero-point energy for the C–H bond is significantly higher than that for the C–D bond, the average distance of the hydrogen from the carbon center is greater than that for deuterium.[31] The other origin of disparities in C–H and C–D bond lengths arises from the relative widths of the ground state C–H and C–D stretching wavefunctions.[32] The smaller reduced mass associated with C–H stretching vibrations translates into a more disperse wave-function. Conceptually, this can be thought of in terms of the lighter particle having more wavelike character than the heavier particle. These two factors, shown in Figure 3, contribute to the C–D bond being shorter than the C–H bond when all other factors are equivalent. This, in turn, translates into the CD_3 group having a smaller effective volume than the CH_3 group.

Early work on steric isotope effects utilized intramolecular conformational changes (Scheme 3) that possess, by design, extremely frustrated transition structures.[33–36] All of these systems yield significant inverse ^{2}H KIEs. Later measurements of steric kinetic isotope effects[37,38] and steric equilibrium isotope effects (EIEs)[39] have also reported inverse values. Also of note is a simple but clever set of recent experiments reported by Dunitz and Ibbertson.[40] Using powder X-ray diffraction measurements, they computed the volume of the unit cells of crystalline C_6H_6 and C_6D_6 at various temperatures and found that C_6H_6 is effectively “larger” than C_6D_6 below 165 K with the trend reversing above 165 K. As the above example suggests, nonbonding interactions other than steric repulsion can contribute to KIEs. Attractive dispersion forces, for example, contribute a normal contribution to observed KIEs and EIEs.[41]

Enantioselective Reductions

To begin our work in looking specifically at mechanistic questions relevant to asymmetric reactions, we approached the stoichiometric DIP-Cl reduction of prochiral ketones in which the mechanism and paradigm for stereoselection were easily apprehendable and well established (Scheme 4).[42–44] In this system, a nominally boatlike, six-membered cyclic transition structure mandates that the small group (R_S) on the prochiral ketone is proximal to the axial methyl group in the participating isopinocampheyl group. To begin this work, we utilized a probe molecule (**1**) that is reduced by DIP-Cl with very high stereoselectivity (>99% enantiomeric excess (*ee*)). The isopropyl substituent, serving as R_S, possesses two prochiral methyl groups. The isopropyl group is an excellent probe substituent, since the prochiral methyl groups are not situated in a way that allows them to donate into an unfilled orbital in the reactant or transition state, thus removing the possible contribution of hyperconjugation to the measured ^{2}H KIE.

The method we employed to measure ^{2}H KIEs at the enantiotopic methyl groups in **1** is shown in Scheme 5.[45] This method utilizes two separate competition experiments to arrive at the desired ^{2}H KIEs at each enantiotopic group. The first competition experiment utilizes a racemic mixture of (*R*)-[D_3]**1** and (*S*)-[D_3]**1** (Scheme 5A). The rate constant ratios are

obtained by performing a high-conversion (≈80–90%) reduction on the racemic mixture. Reisolated starting material is then enriched in the isotopomer that reacts more slowly. Of course, because the isotopic label resides at an enantiotopic position, it is impossible to distinguish the two isotopomers by NMR spectroscopy. To distinguish between the two isotopomers, we perform a desymmetrization using the same highly stereoselective conversion being studied or another conversion that proceeds with high enantioselectivity. In the study of the DIP-Cl reduction, we employed the CBS (Corey–Bakshi–Shibata) reduction as a means of desymmetrizing the reisolated starting material. This choice was based on the fact that the CBS reduction is catalytic and the alcohol product is more easily isolated. After desymmetrization, the previously enantiotopic groups become diastereotopic and can be differentiated by NMR spectroscopy. We often employ ^{1}H NMR spectroscopy to measure the absence of ^{2}H label rather than employing ^{2}H NMR spectroscopy to measure the amount of label in the diastereotopic positions. These measurements provide the ratio of (*R*)-[D_3]**1** to (*S*)-[D_3]**1**. Using Equation (1), we can then compute the rate ratio for the conversion of these two isotopomers from the fractional conversion (*F*) and the ratio of (*R*)-[D_3]**1** to (*S*)-[D_3]**1** in the reisolated starting material (*R*). The resulting rate ratio (KIE_R) can then be expanded into the ratio of the ^{2}H KIEs at each enantiotopic position [Eq. (2)].

$$\frac{k_{(S)\text{-}[D_3]\mathbf{1}}}{k_{(R)\text{-}[D_3]\mathbf{1}}}=\frac{\ln[2(1-F)/(1+1/R)]}{\ln[2(1-F)/(1+R)]} \tag{1}$$

$$\frac{k_{(S)\text{-}[D_3]\mathbf{1}}}{k_{(R)\text{-}[D_3]\mathbf{1}}}=\frac{k_1}{k_{(R)\text{-}[D_3]\mathbf{1}}}/\frac{k_1}{k_{(S)\text{-}[D_3]\mathbf{1}}}=\mathrm{KIE}_R \tag{2}$$

To algebraically abstract the ^{2}H KIEs upon both enantiotopic groups, we need the product of the ^{2}H KIEs at both positions. This can be obtained by using a competition reaction that employs a mixture of **1** and [D_6]**1** (Scheme 5B). The rate ratio for the isotopologues can be obtained (as before) by using a competition reaction. Starting material consisting of a known ratio (R_0) of **1** to [D_6]**1** is taken to high conversion (≈80–90%). The reisolated starting material is then analyzed by using ^{1}H NMR spectroscopy to determine the ratio of **1** to [D_6]**1**. This ratio (*R*), the initial ratio of **1** to [D_6]**1** (R_0), and the fractional conversion (*F*) are then used as inputs into Equation (3) to compute the product KIE, KIE_P. Under the assumption of the rule of the geometric mean, this value is simply the product of the ^{2}H KIEs at each enantiotopic position [Eq. (4)].[46] The final ^{2}H KIEs upon each enantiotopic position can be computed by using the expressions given in Equation (5) and Equation (6). It should be noted that, in principle, it would be possible to obtain KIE_P and KIE_R by measuring fractionation (*R*) in the product of a low conversion reaction. We chose the method above largely because we anticipated that the measured KIEs would be small, and one can achieve substantially greater fractionation in the reisolated reactants in high-conversion reactions than one can in isolated products in low-conversion reactions.[4]

$$\frac{k_1}{k_{[D_6]\mathbf{1}}}=\frac{\ln[(1+1/R_0)(1-F)/(1+1/R)]}{\ln[(1+R_0)(1-F)/(1+R)]} \tag{3}$$

$$\frac{k_1}{k_{[D_6]\mathbf{1}}}=\frac{k_1}{k_{(R)\text{-}[D_3]\mathbf{1}}}\times\frac{k_1}{k_{(S)\text{-}[D_3]\mathbf{1}}}=\mathrm{KIE}_P \tag{4}$$

$$\frac{k_1}{k_{(S)\text{-}[D_3]1}} = \sqrt{KIE_R \times KIE_P} \quad (5)$$

$$\frac{k_1}{k_{(R)\text{-}[D_3]1}} = \sqrt{KIE_P / KIE_R} \quad (6)$$

The resulting ^{2}H KIEs for the DIP-Cl reduction of 4′-methylisobutyrophenone are shown in Figure 4A above a stereoview of the computed transition structure (Figure 4B). Three observations are of note: First, the isopropyl group is oriented toward the axial methyl in the participating isopinocampheyl group. This orientational preference is likely to be mandated by the favorable overlap between the nascent $\sigma_{C–H}$ and the methine $\sigma^*_{C–H}$ orbitals.[47] Or, conversely, stabilization may arise by donation from the methine $\sigma_{C–H}$ orbital into the $\sigma^*_{C–H}$ orbital of the nascent C–H bond.[48] Second, the array of the six actively participating atoms in the transition state is only boatlike in a nominal sense. A more accurate description is that the active atoms undergoing bonding changes in the transition state occupy a nearly planar arrangement. Finally, it can be seen that the pro-*S* methyl on the isopropyl group is in closer proximity to the axial methyl on the participating isopinocampheyl group. This observation is consonant with the more inverse ^{2}H KIE observed at the pro-*S* methyl group. An inverse isotope effect is observed for both enantiotopic methyl groups. This is probably due, in part, to the proximity of the pro-*R* methyl group to one of the 2′-positions on the substrate itself and to the axial methyl group on the participating Ipc. These observations are conceptually self-consistent and emphasize the synergy that can develop from the use of computational and experimental techniques.

Having measured ^{2}H KIEs that appear to result largely from steric interactions, we were determined to extend this approach to ^{13}C KIEs. Steric ^{2}H KIEs result almost exclusively from perturbation of the zero-point energies. Of course, the reduced masses associated with the vibrational manifold of methyl groups include the mass of the carbon atom. It follows that isotopic perturbation of the carbon should result in an observed change in the free energies of activation for different isotopologues. Steric ^{13}C KIEs should be observable. It is questionable, however, how significant these KIEs might be. We designed a method that is similar in intent to that shown in Scheme 5 for the measurement of ^{13}C KIEs at enantiotopic groups.[49] Because these experiments are performed at natural abundance, the technique is less involved than that used to measure ^{2}H KIEs. Scheme 6 illustrates this method. This method is similar in intent and execution to that originally developed and applied by the Singleton[50] research group with one key exception: The stock starting material and reisolated starting material are both desymmetrized prior to quantitative ^{13}C NMR spectroscopic analysis.

The weighted average results from four experiments are shown in Scheme 7A for the DIP-Cl reduction. Scheme 7B shows the ^{13}C KIEs computed from frequencies computed from the optimized transition structure (B3LYP/6–31G*). Not surprisingly, the only substantial KIE resides upon the carbonyl group. However, there is a statistically significant normal ^{13}C KIE upon the pro-*R* methyl position. The absolute value of this result is at variance with expectations, but the trend is in accordance with ^{2}H KIE measurements. Just as the ^{2}H KIE at the pro-*R* position was less inverse (or more normal), the same trend is observed in terms of relative magnitude in the ^{13}C KIEs. There are a number of possible explanations for this behavior. It is possible that there is a polarization effect operative here that is acting upon the $C_{methine}$–$C_{pro\text{-}S}$ and $C_{methine}$–$C_{pro\text{-}R}$ bonds as a result of the delocalization of electron

density occurring near the carbonyl. This polarization effect would result in a loosening of the C–C bonds, thus contributing a normal component to the ^{13}C KIE. It is also quite possible that the full extent of this effect cannot be calculated by using methods that do not accurately account for electron correlation. Another possibility is that dispersion forces are contributing normal components to both the ^{2}H and ^{13}C KIEs. It is possible that this effect is overwhelmed by the inverse steric isotope effect in the case of the ^{2}H KIEs, but is not overwhelmed in the case of the ^{13}C KIEs. It is difficult to determine the origins of this behavior with confidence at this time, since these and measurements upon the CBS reduction (see below) are the only measurements of their kind in existence.

There are, however, some points of conceptual contact with the ^{13}C KIE measurements reported herein and studies upon vibrational frequency shifts observed as a function of pressure. Frequencies corresponding largely to C–C single-bond stretches are almost exclusively blueshifted upon the application of pressure.[51,52] However, heavy-atom bonds with significant dipoles, such as the C–F bond in $CFCl_3$, the C=C bond in CH_2CCl_2, and the C≡N bond in CH_3CN are redshifted over a significant portion of the pressure range explored. Additionally, some multiply bonded C–C stretches experience redshifts upon the application of pressure.[53,54] It is difficult to surmise at present whether these phenomena are the result of polarization effects, but the discordant behavior of single-bonded C–C stretches in ground-state molecules indicates that this is a plausible hypothesis. It is clearly difficult to compare expectations regarding observed frequency shifts under high applied pressure to KIEs reflecting vibrational frequency shifts at the transition state; however, these observations indicate that the potential for other non-bonding interactions to influence observed KIEs exists.

Stereoselection in the CBS reduction system (Scheme 8) is less well understood than in the DIP-Cl case described above.[55,56] Originally conceived by Itsuno et al. as a stoichiometric reductant, the prototype for the CBS catalyst family did not possess a boroalkyl substituent.[57,58] Subsequent addition of a *B*-methyl group by Corey and co-workers resulted primarily in an increase in catalyst stability.[59] Further modifications of the boroalkyl substituent did little to affect stereoselection in the reduction of a common test substrate for this reduction, acetophenone.[60,61] Replacement of the prolinol substituents, however, did have substantial effects upon stereoselection in the reduction of acetophenone[56,61] A final way in which stereoselection can be controlled is by the variation of the stoichiometric reductant. This modification presumably works through limiting the nonselective background reduction.

We measured ^{2}H[62] and ^{13}C[63] KIEs in the CBS reduction system to better understand the way in which stereoselection is accomplished. Once again, we employed a probe molecule (**3**) in which the small substituent was an isopropyl group. The aromatic group was chosen such that stereoselectivity was very high (>99% *ee*) so that isotopic fractionation results almost exclusively from a single transition state. A weighted average of three determinations of ^{2}H KIEs are shown in Figure 5A. A stereoview of the favored *Si*-attack transition structure (B3LYP/6–31 + G(d,p)) possessing a boatlike arrangement of atoms undergoing bonding changes is shown in Figure 5B. Arrangements of groups near the pro-*S* and pro-*R* methyl groups are shown in Figure 6A and B.

Several conclusions may be drawn from the computed transition structure and the measured KIEs. First, unlike the DIP-Cl reduction system, the nascent C–H bond is not antiperiplanar to the methine C–H bond in the isopropyl group in the computed transition structure. It appears that this electronically favorable arrangement is at variance with repulsive steric interactions that would be imposed by the *B*-methyl group under such an arrangement. Furthermore, it appears that the pro-*S* methyl group, which experiences a substantial

inverse ^{2}H KIE, is proximal to the *B*-methyl group. These observations are at some variance with the observation that changes in the boroalkyl substituent do not affect enantioselectivity in the reduction of acetophenone. However, it is clear that 2′,5′-dimethylisobutyrophenone makes different demands upon the organization of the transition state. From the transition structure, it can be seen that prolinol groups and the boroalkyl group may have a role in stereoselection. Perhaps one of the most surprising observations is that prohibition of the antiperiplanar arrangement of the nascent C–H bond and the methine C–H bond forces the pro-*R* methyl group to interact with the aryl substituent in the ketone. In fact, the interactions of the pro-*R* methyl group with the 6′-position and the incoming BH_3 are believed to give rise to the dominant inverse ^{2}H KIE observed in the pro-*R* position. Finally, the fact that this stabilizing orbital interaction is observed in the DIP-Cl transition state, but not the CBS transition state means speaks to the delicate balance that exists between electronic and steric effects in stereoselective reactions.

Measurements of ^{13}C KIEs for the (*S*)-Me-CBS-catalyzed reduction of **3** are shown in Scheme 9 as weighted averages of four measurements. As was observed in the DIP-Cl system, the KIEs at the enantiotopic groups are not inverse and, in fact, do not differ significantly from unity. This seems surprising in light of the fact that the inverse ^{2}H KIE at the pro-*R* position was substantial. Observation of the same trends in measured ^{13}C KIEs that are normal or nonexistent in positions where substantial inverse ^{2}H KIEs were observed serves to highlight the need for a more intensive look at the origins of these subtle effects. As instrumentation and methods improve, subtle contributions to KIEs may serve to better understand the physical processes that accompany stereoselection.

The experiments described above have begun to shed new light on exactly how steric interactions enforce stereochemistry and how these interactions manifest themselves as experimental observables. However, these studies have presented us with a host of unanswered questions that span from the natures and relative strengths of various nonbonding interactions to questions regarding effective paradigms for successful asymmetric reagent and catalyst design.

Organocatalysis

Organocatalysis has been one of the most rapidly growing areas of recent synthetic methodology development.[64] Perhaps one of the most intriguing examples is that of the archetypical proline-catalyzed intramolecular aldol reaction (Scheme 10).[65,66] Numerous mechanistic proposals have been forwarded since the first report of this reaction. Likewise, investigations of stereoselection in this reaction has spawned interesting arguments regarding the possible involvement of two (or more) proline molecules in the product-determining step.[67,68] Excellent work by the Houk,[69,70] List,[71] and Blackmond[72] groups have resolved the question and find no cogent argument for the participation of more than one proline. Of course, in asymmetric catalysis, reactivity provides an important counterpoint to selectivity. In most aldol and related reactions, C–C bond formation is presumed to be rate limiting. We began our investigations into the intramolecular proline-catalyzed aldol reaction with the hypothesis that C–C bond formation was at least partially rate determining. This hypothesis was based on the calculations of Houk and co-workers, who computed the entire reaction pathway for this reaction and found that, without the inclusion of a solvent model, enamine formation and C– C bond formation were likely to be partially rate limiting.[70] It is reasonable to assume that, if C–C bond formation was partially or fully rate limiting, the ^{13}C KIEs at each enantiotopic carbonyl on **5** would be substantially different. This appeared to be the perfect system in which to use our method for measuring ^{13}C KIEs at enantiotopic positions.

We measured ^{13}C KIEs upon **5** using the conventional Singleton method and our method in which the reisolated starting material is desymmetrized prior to quantitative ^{13}CNMR spectroscopic analysis.[73] Surprisingly, we found no appreciable ^{13}C KIE at either prochiral carbonyl. In fact, the only position with a substantial ^{13}C KIE was the acyclic carbonyl (Scheme 11). The implications of this finding are that the environments of the pro-*R* and pro-*S* carbonyls are not appreciably different until after the rate-determining step. The absence of a ^{13}C KIE at the methyl group adjacent to the acyclic carbonyl implies further that enamine formation is not rate limiting. This limits candidates for the rate-determining step to carbinolamine formation (Scheme 12A) or iminium formation (Scheme 12B). The key C–C bondformation step (Scheme 12C) is clearly excluded by the experimental KIEs.

Calculations of ^{13}C KIEs computed from (B3LYP/6–31 + G(d,p)) optimized transition structures for carbinolamine formation, iminium formation, and C–C bond formation resulted in the KIEs shown in Scheme 13 A–C, respectively. These calculations utilized an IEFPCM model for solvent.[74] The calculations agree closely with the measured values. However, unfortunately, they do not lead to a clear preference for the rate-limiting step. We are currently performing kinetic measurements to discern between the two tenable candidates for rate-limiting step.

The surprising findings described above have naturally led to questions of whether C–C bond formation is rate limiting in intermolecular proline-catalyzed aldol reactions. Blackmond and co-workers recently reported a study that suggests that C–C bond formation is, in fact, rate limiting in the intermolecular proline-catalyzed aldol.[75] These findings are not entirely surprising, considering that the effective concentration of the nucleophilic enamine in the intramolecular reaction should substantially lower the free energy of activation for C–C bond formation. As future organocatalytic strategies evolve for the transfer of chirality, simultaneous control of reactivity and selectivity will continue to be important design features. Our work on the intramolecular proline-catalyzed reaction represents a link in a continuous chain of valuable mechanistic work in this area. As organocatalysis continues to develop, it is important that a dialogue is established between the fields of synthetic methodology and mechanistic organic chemistry.

Summary and Outlook

We have illustrated some of the considerations that one must bear in mind when tailoring the development of mechanistic tools to questions involving stereochemistry. Likewise, we have illustrated two KIE methodologies that are, in conjunction with computational work and other kinetic treatments, capable of probing the process of stereoselection. While these methods have only recently come into being and have been applied to only a few systems, trends are emerging. We have begun to understand the magnitudes of observable ^{2}H KIEs that appear to result from steric interactions. We have gained some insight into difficulties surrounding the calculation of steric ^{2}H KIEs from harmonic force constant calculations. And, we have started to calibrate the fine energetic balance between steric and electronic directing forces. As the methods described within are applied to a broader range of systems, our understanding of the physical process of stereoselection will become deeper, which allows more facile design of new stereoselective reactions.

The synergy between computational chemistry and KIE studies cannot be overstated. Comparisons between computed and experimental ^{13}C KIEs offer unique opportunities to validate transition-structure models. In the asymmetric reductions studied herein, we have started to understand how experimentally validated transition structures differ from canonical chair- and boatlike transition structures. We have also begun to comprehend the distance scale at which steric interactions occur in these reactions. We have also uncovered

surprising aspects of reactivity in the intramolecular proline-catalyzed aldol reaction. The effective concentration of the enamine nucleophile about the electrophilic carbonyl appears to lower the free energy of activation to a level that removes this step from participation in rate determination.

As the mechanistic investigation of asymmetric reactions progresses, ways of expanding the scope of traditional mechanistic methods, such as linear free energy relationships to elucidate mechanistic features of asymmetric reactions can also be expected to play a key role. The Sigman research group[76–79] (among others[80]) has been active in using linear free energy relationships to probe asymmetric reactions. New enabling technologies also promise to facilitate future mechanistic work. Given the prominent role of nonbonding interactions in determining the stereochemical course of a reaction, new density functionals that contain corrections for nonbonding interactions will aid in meaningful comparisons of experimental and computational work.[81–83] Likewise, the development of cryoprobes can be expected to aid NMR spectroscopy based studies of reaction mechanism. Bennet and co-workers have applied cryoprobes to great effect to achieve in situ monitoring of reaction progress as a function of isotopic label in enzymes.[84] The creative expansion of classical methods and the development of enabling technologies promises to facilitate mechanistic study spanning the gamut from asymmetric small molecule reactions to enzyme-catalyzed reactions.

The opportunities are nearly endless for the application of the methods reviewed herein. As new forays are made into challenging stereoselective reactions, the need to understand the physical processes at work grows. Our future efforts will be shaped by two guiding principles: 1) the intent to understand KIEs in terms of the physical forces that are operative at the transition state and 2) the intent to aid the development of new stereoselective reactions. First, we seek to understand the physical origins of isotope effects that originate from nonbonding forces. These efforts will rely upon further experimentation and the development of new methods for the reliable calculation of steric ^{2}H KIEs. We intend to look at systems in which extreme steric demands develop at the transition state. These studies seek to determine the conditions necessary to measure ^{13}C KIEs that unequivocally originate from steric repulsion. We also plan to develop corrections for vibrations that are impacted by steric repulsion based on calculations designed to probe the effects of anharmonicity upon vibrational energy levels. Fulfillment of our second broad goal will involve the development of general techniques that are capable of measuring KIEs that result from both major and minor reaction pathways. This feature will make the new technique applicable to reactions in which only moderate stereoselectivity is observed. Experimentally validated computational models can then be used to aid future reaction design efforts. The development of new stereoselective reactions has always depended upon mechanistic insight. We hope that the mechanistic methods described herein and those currently being developed will foster an even more productive partnership between mechanism and synthetic methodology.

Acknowledgments

We thank the NIGMS (GM87706-01) and the PRF (48060-G4) for funding and the National Science Foundation for computational resources through TeraGrid access provided by PSC. We also thank Charlie Perrin (UCSD) for the suggestion of the sumo match as a contest in which the more massive participant is likely to win.

References

1. Recent examples: a) McCusker KP, Klinman JP. J. Am. Chem. Soc 2010;132:5114–5120. [PubMed: 20302299] b) Findlater M, Bernskoetter WH, Brookhart M. J. Am. Chem. Soc 2010;132:4534–4535. [PubMed: 20232913] c) Yasutomi Y, Suematsu H, Katsuki T. J. Am. Chem. Soc

2010;132:4510–4511. [PubMed: 20232868] d) Yang X, Zhao L, Fox T, Wang Z-X, Berke H. Angew. Chem. Int. Ed 2010;49:2058–2062. e) Leow D, Lin S, Chittimalla SK, Fu X, Tan C-H. Angew. Chem 2008;120:5723–5727. Angew. Chem. Int. Ed 2008;47:5641–5645. f) Chan W-W, Yeung S-H, Zhou Z, Chan ASC, Yu W-Y. Org. Lett 2010;12:604–607. [PubMed: 20043644] g) Wong FM, Wang J, Hengge AC, Wu W. Org. Lett 2007;9:1663–1665. [PubMed: 17408276] h) Edwards DR, Montoya-Peleaz P, Crudden CM. Org. Lett 2007;9:5481–5484. [PubMed: 18041844] i) Stowers KJ, Sanford MS. Org. Lett 2009;11:4584–4587. [PubMed: 19754074] j) Sun K, Sachwani R, Richert KJ, Driver TG. Org. Lett 2009;11:3598–3601. [PubMed: 19627144]

2. Recent examples: a) Mugridge JS, Bergman RG, Raymond KN. Angew. Chem 2010;122:3717–3719. Angew. Chem. Int. Ed 2010;49:3635–3637. b) Penoni A, Palmisano G, Zhao Y-L, Houk KN, Volkman J, Nicholas KM. J. Am. Chem. Soc 2009;131:653–661. [PubMed: 19093864] c) Luo M, Schramm VL. J. Am. Chem. Soc 2008;130:11617–11619. [PubMed: 18693725] d) Spies MA, Toney MD. J. Am. Chem. Soc 2007;129:10678–10685. [PubMed: 17691728] e) Bailey BC, Fan H, Huffman JC, Baik M-H, Mindiola DJ. J. Am. Chem. Soc 2007;129:8781–8793. [PubMed: 17592842] f) Seo SY, Marks TJ. Chem. Eur. J 2010;16:5148–5162. g) Lu Y, Qu F, Zhao Y, Small AMJ, Bradshaw J, Moore B. J. Org. Chem 2009;74:6503–6510. [PubMed: 19670893] h) Brinker UH, Lin G, Xu L, Smith WB, Mieusset J-L. J. Org. Chem 2007;72:8434–8451. [PubMed: 17918998]

3. Recent examples: a) Schneider N, Finger M, Haferkemper C, Bellemin-Laponnaz S, Hofmann P, Gade LH. Angew. Chem 2009;121:1637–1641. Angew. Chem. Int. Ed 2009;48:1609–1613. b) McCann JAB, Berti PJ. J. Am. Chem. Soc 2008;130:5789–5797. [PubMed: 18393424] c) McCann JAB, Berti PJ. J. Am. Chem. Soc 2007;129:7055–7064. [PubMed: 17497857] d) Zhang Y, Luo M, Schramm VL. J. Am. Chem. Soc 2009;131:4685–4694. [PubMed: 19292447] e) Hirschi JS, Takeya T, Hang C, Singleton DA. J. Am. Chem. Soc 2009;131:2397–2403. [PubMed: 19146405] f) Kelly KK, Hirschi JS, Singleton DA. J. Am. Chem. Soc 2009;131:8382–8383. [PubMed: 19485324] g) Oyola Y, Singleton DA. J. Am. Chem. Soc 2009;131:3130–3131. [PubMed: 19215077] h) Thomas JB, Waas JR, Harmata M, Singleton DA. J. Am. Chem. Soc 2008;130:14544–14555. [PubMed: 18847260] i) Christian CF, Takeya T, Szymanski MJ, Singleton DA. J. Org. Chem 2007;72:6183–6189. [PubMed: 17608437]

4. Melander, L.; Saunders, WH, Jr. Reaction Rates of Isotopic Molecules. Malabar: Krieger Publishing; 1987.

5. Recent applications of primary KIEs to tunneling phenomena: a) Panay AJ, Fitzpatrick PF. J. Am. Chem. Soc 2010;132:5584–5585. [PubMed: 20355730] b) Yoon M, Song H, Håkansson K, Marsh ENG. Biochemistry 2010;49:3168–3173. [PubMed: 20225826] c) Zhang X, Datta A, Hrovat DA, Borden WT. J. Am. Chem. Soc 2009;131:16002–16003. [PubMed: 19831346] d) Wong K-Y, Richard JP, Gao J. J. Am. Chem. Soc 2009;131:13963–13971. [PubMed: 19754046] e) Tsang W-Y, Richard JP. J. Am. Chem. Soc 2009;131:13952–13962. [PubMed: 19788330] f) Wu A, Mader EA, Datta A, Hrovat DA, Borden WT, Mayer JM. J. Am. Chem. Soc 2009;131:11985–11997. [PubMed: 19618933] g) Sharma SC, Klinman JP. J. Am. Chem. Soc 2008;130:17632–17633. [PubMed: 19061319]

6. Reviews: a) Hammes-Schiffer S. Acc. Chem. Res 2006;39:93–100. [PubMed: 16489728] b) Truhlar DG, Gao J, Alhambra C, Garcia-Viloca M, Corchado J, Sánchez ML, Villa J. Acc. Chem. Res 2002;35:341–349. [PubMed: 12069618] c) Kohen A, Klinman JP. Acc. Chem. Res 1998;31:397–404. d) Kwart H. Acc. Chem. Res 1982;15:401–408. e) Huynh MHV, Meyer TJ. Chem. Rev 2007;107:5004–5064. [PubMed: 17999556] f) Fernández-Ramos A, Miller JA, Klippenstein StJ, Truhlar DG. Chem. Rev 2006;106:4518–4584. [PubMed: 17091928] g) Nagel ZD, Klinman JP. Chem. Rev 2006;106:3095–3118. [PubMed: 16895320] h) Antoniou D, Basner J, Núñez S, Schwartz SD. Chem. Rev 2006;106:3170–3187. [PubMed: 16895323] i) Pu J, Gao, Donald J, Truhlar G. Chem. Rev 2006;106:3140–3169. [PubMed: 16895322] j) Caldin EF. Chem. Rev 1969;69:135–156. k) Weston, RE, Jr. Isotopes and Chemical Principles. Peter, R., editor. Washington: ACS; 1975. p. 44-63.

7. a) Ussing BR, Hang C, Singleton DA. J. Am. Chem. Soc 2006;128:7594–7607. [PubMed: 16756316] b) Thomas JB, Waas JR, Harmata M, Singleton DA. J. Am. Chem. Soc 2008;130:14544–14555. [PubMed: 18847260] c) Oyola Y, Singleton DA. J. Chem. Am. Soc 2009;131:3130–3131.

8. Westheimer FH. Chem. Rev 1961;61:265–273.

9. Recent examples: a) Iyer S, Hengge AC. J. Org. Chem 2008;73:4819–4829. [PubMed: 18533704] b) Marlier JF, Fogle EJ, Cleland WW. Biochemistry 2008;47:11158–11163. [PubMed: 18817416] c) Lin Y, Volkman J, Nicholas KM, Yamamoto T, Eguchi T, Nimmo SL, West AH, Cook PF. Biochemistry 2008;47:4169–4180. [PubMed: 18321070] d) Humphry T, Iyer S, Iranzo O, Morrow JR, Richard JP, Paneth P, Hengge AC. J. Am. Chem. Soc 2008;130:17858–17866. [PubMed: 19053445] e) Ashley DC, Brinkley DW, Roth JP. Inorg. Chem 2010;49:3661–3675. [PubMed: 20380467] f) Dai Q, Frederiksen JK, Anderson VE, Harris ME, Piccirilli JA. J. Org. Chem 2008;73:309–311. [PubMed: 18052189] g) Dybala-Defratyka A, Szatkowski L, Kaminski R, Wujec M, Siwek A, Paneth P. Environ. Sci. Technol 2008;42:7744–7750. [PubMed: 19031855]
10. Bartell LS. J. Am. Chem. Soc 1961;83:3567–3571.
11. Shiner VJ Jr. Tetrahedron 1959;5:243–252.
12. Kirsch, JF. Isotope Effects on Enzyme-Catalyzed Reactions. Cleland, WW.; O'Leary, MH.; Northrop, DB., editors. Baltimore: University Park Press; 1977. p. 100-121.
13. Gajewski JJ, Olson LP, Tupper KJ. J. Am. Chem. Soc 1993;115:4548–4553.
14. Garrett BC, Truhlar DG. J. Am. Chem. Soc 1980;102:2559–2570.
15. Truhlar DG. Annu. Rev. Phys. Chem 1984;35:159–189.
16. Quapp W, Kraka E, Cremer D. J. Phys. Chem. A 2007;111:11287–11293. [PubMed: 17705351]
17. Grote RF, Hynes JT. J. Chem. Phys 1980;73:2715–2732.
18. Higashi M, Hayashi S, Kato S. J. Chem. Phys 2007;126:144503-1–144503-10. [PubMed: 17444719]
19. Gruber-Stadler M, Muhlhauser M, Sellevåg SR, Nielsen CJ. J. Phys. Chem. A 2008;112:9–22. [PubMed: 18069803]
20. Marinkovic M, Gruber-Stadler M, Nicovich JM, Soller R, Mühlhäuser M, Wine PH, Bache-Andreassen L, Nielsen CJ. J. Phys. Chem. A 2008;112:12416–12429. [PubMed: 18989948]
21. Evans DA, Vogel E, Nelson JV. J. Am. Chem. Soc 1979;101:6120–6123.
22. Vittorelli P, Winkler T, Hansen H-J, Schmid H. Helv. Chim. Acta 1968;51:1457–1461.
23. Roush WR. J. Org. Chem 1991;56:4151–4157.
24. Zimmerman HE, Traxler MD. J. Am. Chem. Soc 1957;79:1920–1923.
25. Cram DJ, Elhafez FAA. J. Am. Chem. Soc 1952;74:5828–5835.
26. Chérest M, Felkin H, Prudent N. Tetrahedron Lett 1968;9:2199–2204.
27. Cornforth JW, Cornforth MRH, Mathew KK. J. Chem. Soc 1959:112–127.
28. a) Leitereg TJ, Cram DJ. J. Am. Chem. Soc 1968;90:4011–4018. b) Leitereg TJ, Cram DJ. J. Am. Chem. Soc 1968;90:4019–4026.
29. Reetz MT, Kesseler K, Jung A. Tetrahedron Lett 1984;25:729–732.
30. Evans DA, Dart MJ, Duffy JL, Yang MG. J. Am. Chem. Soc 1996;118:4322–4343.
31. Carter RE, Melander L. Adv. Phys. Org. Chem 1973;10:1–23.
32. Gelabert R, Moreno M, Lluch JM. J. Phys. Chem. A 2009;113:14161–14169. [PubMed: 19928891]
33. Mislow K, Graeve R, Gordon AJ, Wahl GH. J. Am. Chem. Soc 1964;86:1733–1741.
34. Carter RE, Dahlgren L. Acta Chem. Scand 1969;23:504–514.
35. Melander L, Carter RE. J. Am. Chem. Soc 1964;86:295–296.
36. Sherrod SA, da Costa RL, Barnes RA, Boekelheide V. J. Am. Chem. Soc 1974;96:1565–1577.
37. Felder T, Schalley CA. Angew. Chem 2003;115:2360–2363.Angew. Chem. Int. Ed 2003;42:2258–2260.
38. Hayama T, Baldridge KK, Wu Y-T, Linden A, Siegel JS. J. Am. Chem. Soc 2008;130:1583–1591. [PubMed: 18193866]
39. Saunders M, Wolfsberg M, Anet FAL, Kronja O. J. Am. Chem. Soc 2007;129:10276–10281. [PubMed: 17655301]
40. Dunitz JD, Ibbertson RM. Angew. Chem 2008;120:4276–4278.Angew. Chem. Int. Ed 2008;47:4208–4210.
41. Turowski M, Yamakawa N, Meller J, Kimata K, Ikegami T, Hosoya K, Tanaka N, Thornton ER. J. Am. Chem. Soc 2003;125:13836–13849. [PubMed: 14599224]

42. Chandrasekharan J, Ramachandran PV, Brown HC. J Org. Chem 1985;50:5445–5450.
43. Brown HC, Chandrasekharan J, Ramachandran PV. J. Am. Chem. Soc 1988;110:1539–1546.
44. Ramachandran PV, Gong B, Brown HC, Francisco JS. Tetrahedron Lett 2004;45:2603–2605.
45. West JD, Stafford SE, Meyer MP. J. Am. Chem. Soc 2008;130:7816–7817. [PubMed: 18517199]
46. Decius JC, Wilson EB Jr. J. Chem. Phys 1951;19:1409–1412.
47. Cherest M, Felkin H. Tetrahedron Lett 1968;9:2205–2208.
48. Cieplak AS. J. Am. Chem. Soc 1981;103:4540–4552.
49. Stafford SE, Meyer MP. Tetrahedron Lett 2009;50:3027–3030.
50. Singleton DA, Thomas AA. J. Am. Chem. Soc 1995;117:9357–9358.
51. Schindler W, Jonas J. J. Chem. Phys 1980;73:3547–3552.
52. Lee M-R, Ben-Amotz D. J. Chem. Phys 1993;99:10074–10077.
53. Benson AM Jr, Drickamer HG. J. Chem. Phys 1957;27:1164–1174.
54. Wiederkehr RR, Drickamer HG. J. Chem. Phys 1958;28:311–316.
55. Corey EJ, Bakshi RK, Shibata S. J. Am. Chem. Soc 1987;109:5551–5553.
56. Corey EJ, Helal CJ. Angew. Chem 1998;110:2092–2118.Angew. Chem. Int. Ed 1998;37:1986–2012.
57. Itsuno S, Ito K. J. Org. Chem 1984;49:555–557.
58. Itsuno S, Ito K, Hirao A, Nakamura S. J. Chem. Soc. Chem. Commun 1983:469–470.
59. Corey EJ, Bakshi RK, Shibata S, Chen C-P, Singh VK. J. Am. Chem. Soc 1987;109:7925–7926.
60. Corey EJ, Link JO. Tetrahedron Lett 1992;33:4141–4144.
61. Corey EJ, Link JO. Tetrahedron Lett 1989;30:6275–6278.
62. Meyer MP. Org. Lett 2009;11:4338–4341. [PubMed: 19775183]
63. Saavedra J, Stafford SE, Meyer MP. Tetrahedron Lett 2009;50:1324–1327.
64. Reviews: a) Jarvo ER, Miller SJ. Tetrahedron 2002;58:2481–2495. b) List B. Tetrahedron 2002;58:5573–5590. c) Dalko PI, Moisan L. Angew. Chem 2004;116:5248–5286. Angew. Chem. Int. Ed 2004;43:5138–5175. d) Notz W, Tanaka F, Barbas CF III. Acc. Chem. Res 2004;37:580–591. [PubMed: 15311957] e) List B. Acc. Chem. Res 2004;37:548–557. [PubMed: 15311954] f) Seayad J, List B. Org. Biomol. Chem 2005;3:719–724. [PubMed: 15731852] g) Taylor MS, Jacobsen EN. Angew. Chem 2006;118:1550–1573. Angew. Chem. Int. Ed 2006;45:1520–1543. h) Stephen JC. Chem. Eur. J 2006;12:5418–5427. i) Mukherjee S, Yang JW, Hoffman S, List B. Chem. Rev 2007;107:5471–5569. [PubMed: 18072803] j) Pellissier H. Tetrahedron Lett 2007;48:9267–9331. k) Bertelsen S, Jørgensen KA. Chem. Soc. Rev 2009;38:2178–2189. [PubMed: 19623342]
65. Eder U, Sauer G, Wiechert R. Angew. Chem 1971;83:492–493.Angew. Chem. Int. Ed. Engl 1971;10:496–497.
66. Hajos ZG, Parrish DR. J. Org. Chem 1974;39:1615–1621.
67. Puchot C, Samuel O, Duñach E, Zhao S, Agami C, Kagan HB. J. Am. Chem. Soc 1986;108:2353–2357.
68. Agami C, Puchot C. J. Mol. Catal 1986;38:341–343.
69. Allemann C, Gordillo R, Clemente FR, Cheong PH-Y, Houk KN. Acc. Chem. Res 2004;37:558–569. [PubMed: 15311955]
70. Clemente FR, Houk KN. Angew. Chem 2004;116:5890–5892.Angew. Chem. Int. Ed 2004;43:5766–5768.
71. List B, Hoang L, Martin HJ. Proc. Natl. Acad. Sci. USA 2004;101:5839–5842. [PubMed: 15073330]
72. Klussmann M, Iwamura H, Mathew SP, Wells DH Jr, Pandya U, Armstrong A, Blackmond DG. Nature 2006;441:621–623. [PubMed: 16738656]
73. Zhu H, Clemente FR, Houk KN, Meyer MP. J. Am. Chem. Soc 2009;131:1632–1633. [PubMed: 19191687]
74. Tomasi J, Mennucci B, Cammi R. Chem. Rev 2005;105:2999–3094. [PubMed: 16092826]

75. Zotova N, Broadbelt LJ, Armstrong A, Blackmond DG. Bioorg. Med. Chem. Lett 2009;19:3934–3937. [PubMed: 19362473]
76. Jensen KH, Sigman MS. Angew. Chem 2007;119:4832–4834.Angew. Chem. Int. Ed 2007;46:4748–4750.
77. Miller JJ, Sigman MS. Angew. Chem 2008;120:783–786.Angew. Chem. Int. Ed 2008;47:771–774.
78. Sigman MS, Miller JJ. J. Org. Chem 2009;74:7633–7643. [PubMed: 19813764]
79. Gustafson JL, Sigman MS, Miller SJ. Org. Lett 2010;12:2794–2797. [PubMed: 20486656]
80. Zhu H, Reyes NS, Meyer MP. Tetrahedron Lett 2009;50:6803–6806.
81. Zhao Y, Truhlar DG. Theor. Chem. Acc 2008;120:215–241.
82. Zhao Y, Truhlar DG. J. Phys. Chem. A 2006;110:5121–5129. [PubMed: 16610834]
83. Grimme S. J. Comput. Chem 2006;27:1787–1799. [PubMed: 16955487]
84. Chan J, Lewis AR, Gilbert M, Karwaski M-F, Bennet AJ. Nat. Chem. Biol 2010;6:405–407. [PubMed: 20418878]

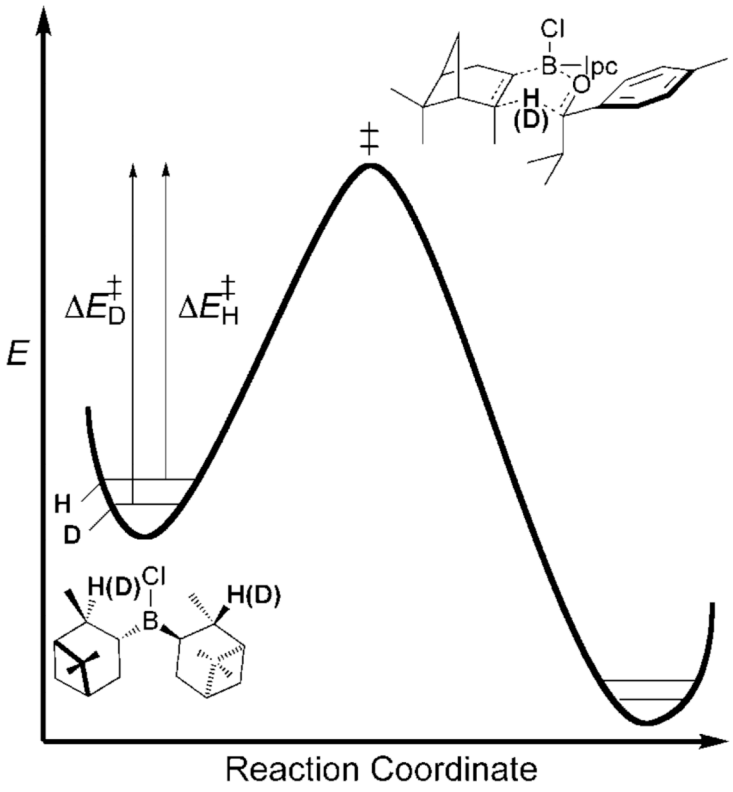

Figure 1.
Simple model for primary ^{2}H KIEs resulting from differences in zero-point energy in the reactants.

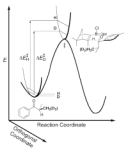

Figure 2.
Simple model for secondary ^{2}H KIEs resulting from differences in zero-point energy in a vibrational coordinate that is orthogonal to the reaction coordinate.

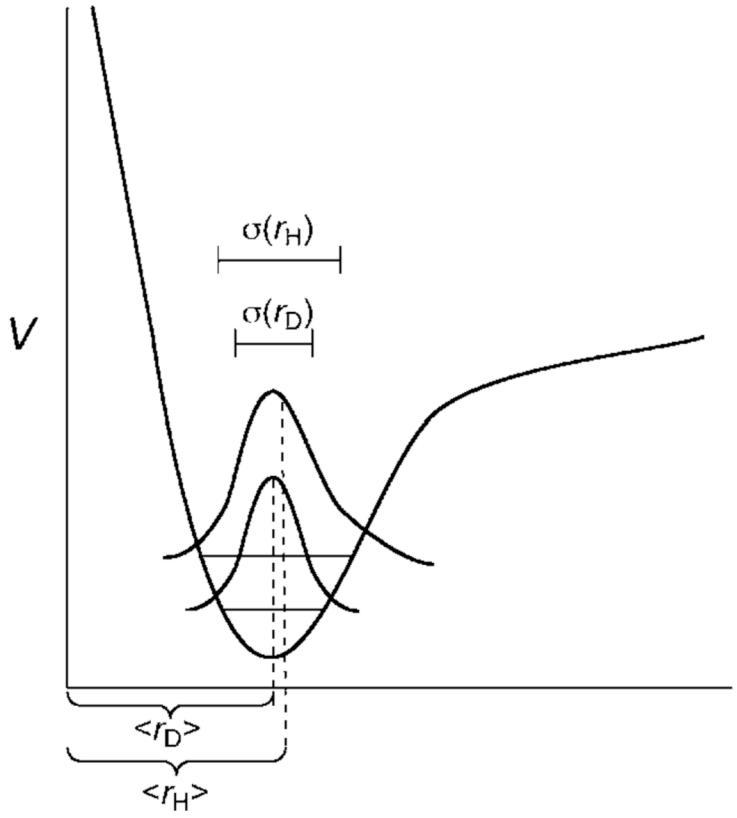

Figure 3.
Anharmonicity in C–H(D) bonds results in the C–H bond having a greater steric presence through differences in average bond length (<*r*>) and differences in wavefunction dispersion, σ(*r*). Offset of $<r_D>$ from the peak of the probability distribution for the C–D bond is the result of asymmetry due to increased sampling of the more anharmonic part of the potential.

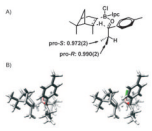

Figure 4.
A) ^{2}H KIEs measured for the (–)-DIP-Cl reduction of 4′-methylisobutyrophenone. B) Stereoview of the computed transition structure for the same reaction.

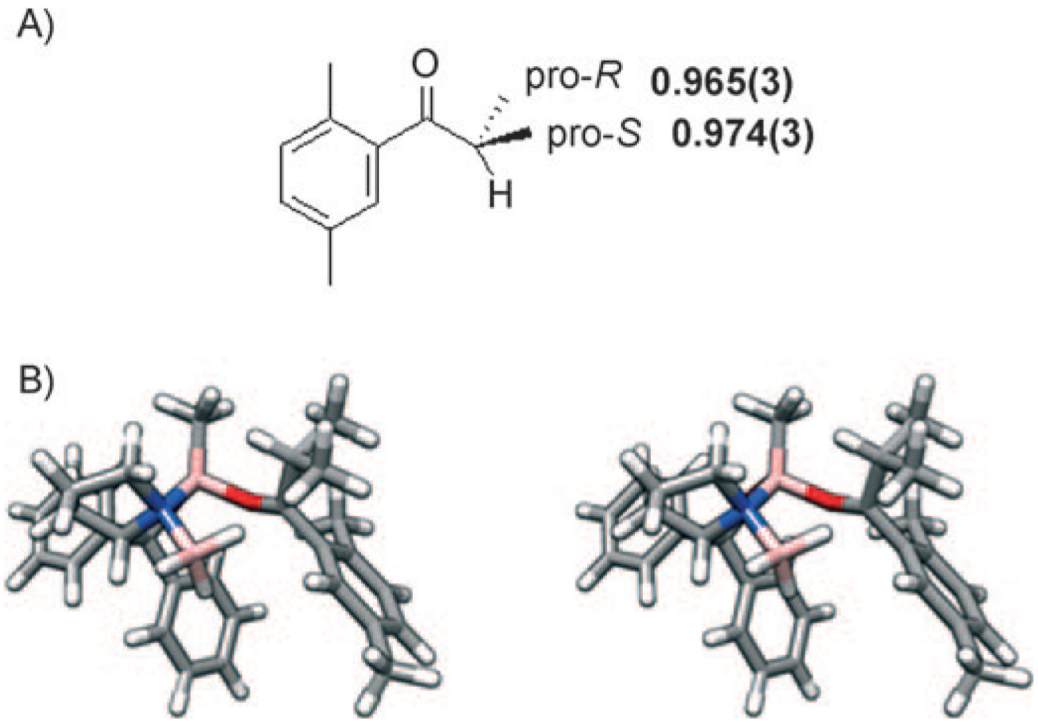

Figure 5.
A) ^{2}H KIEs measured for the (*S*)-Me-CBS-catalyzed reduction of 2′,5′-dimethylisobutyrophenone. B) Stereoview of the computed transition structure for the same reaction, including the BH_3 reductant coordinated to the (*S*)-Me-CBS catalyst.

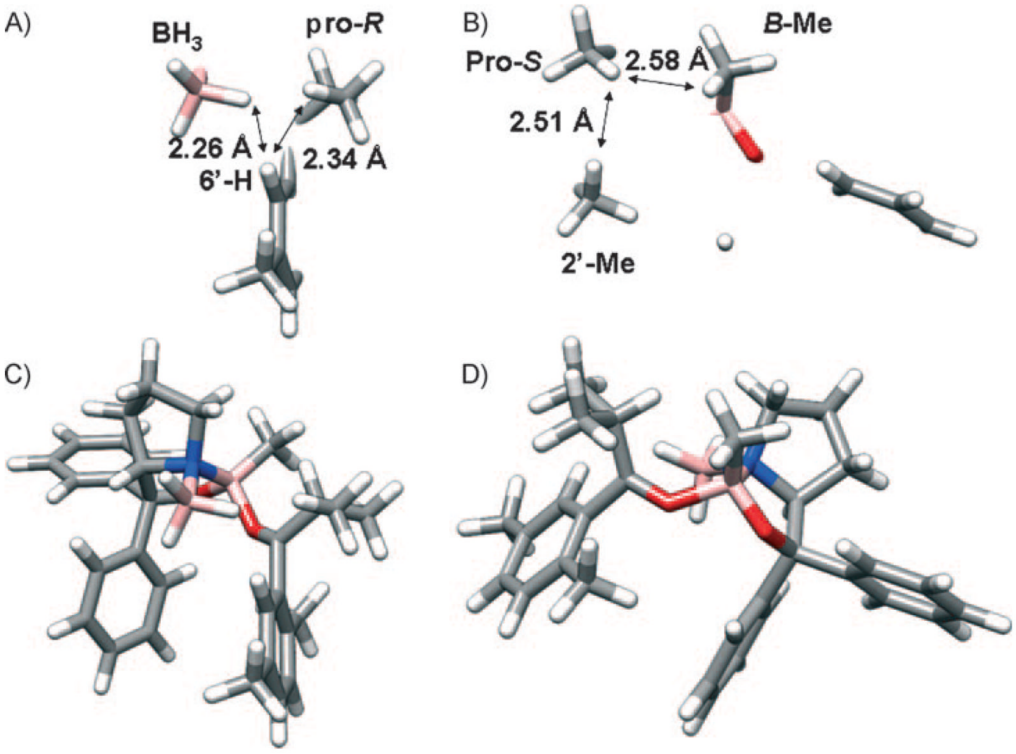

Figure 6.
Nearest neighbor interactions of the A) pro-*S* and B) pro-*R* methyl groups at the CBS reduction transition state. Distances denote closest H–H contacts. Full transition structures corresponding to the arrangements in A and B are shown in C and D, respectively.

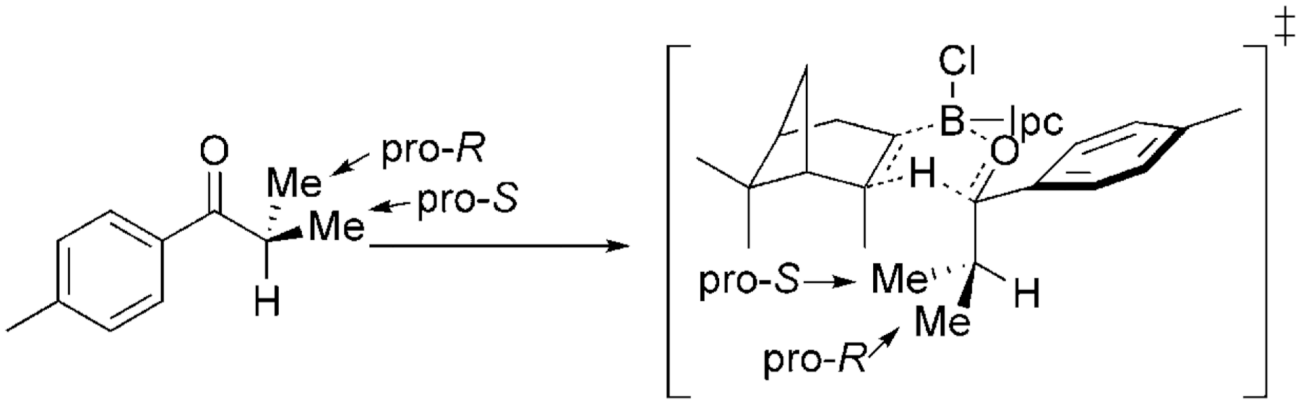

Scheme 1.

Groups that are enantiotopic in the reactant become diastereotopic in the transition state, such as in this DIP-Cl (*B*-chlorodiisopino-campheylborane) reduction example. IPc= isopinocampheyl.

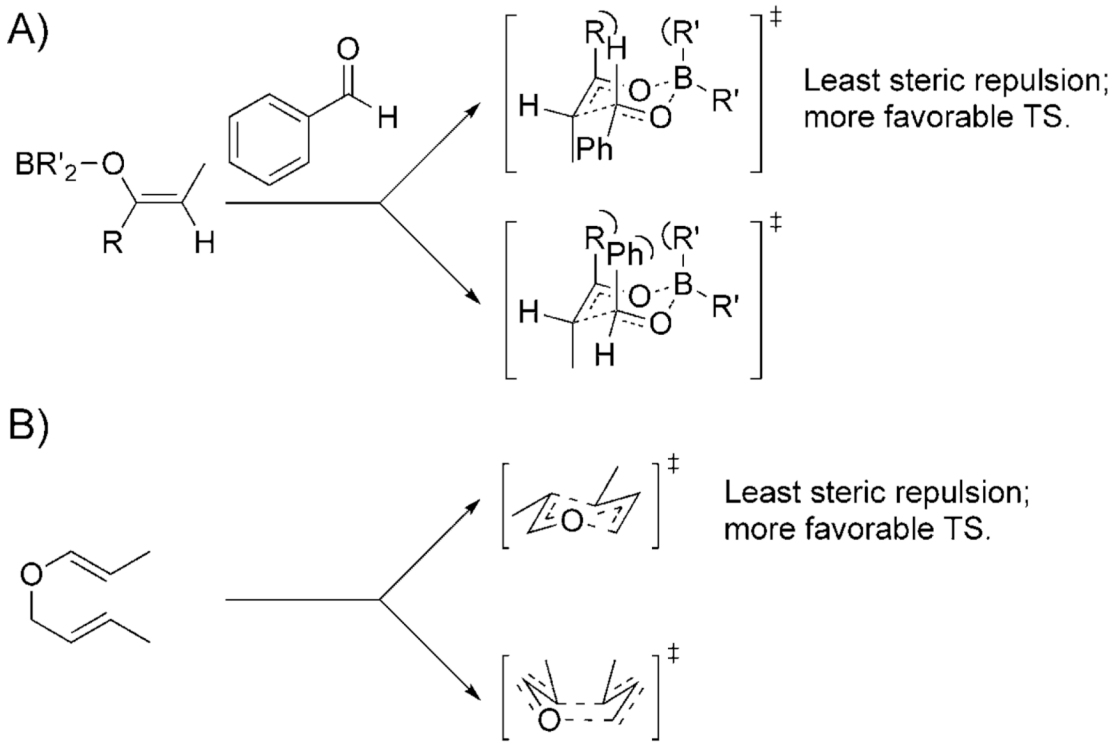

Scheme 2.

Model transition structures for major and minor stereochemical pathways in A) aldol reactions using *Z*-boron enolates as nucleophiles and B) a Claisen rearrangement. TS=transition state.

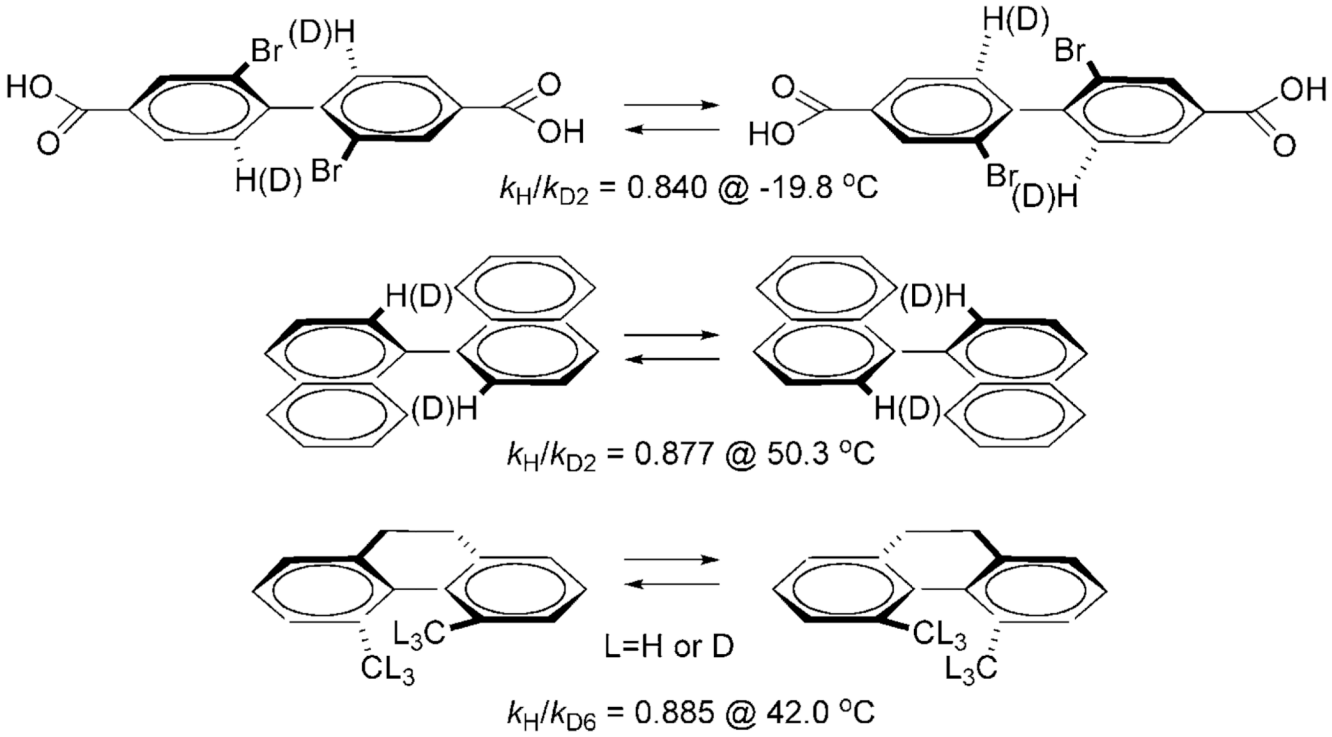

Scheme 3.
Steric ^{2}H KIEs measured in classic systems are significant and inverse.

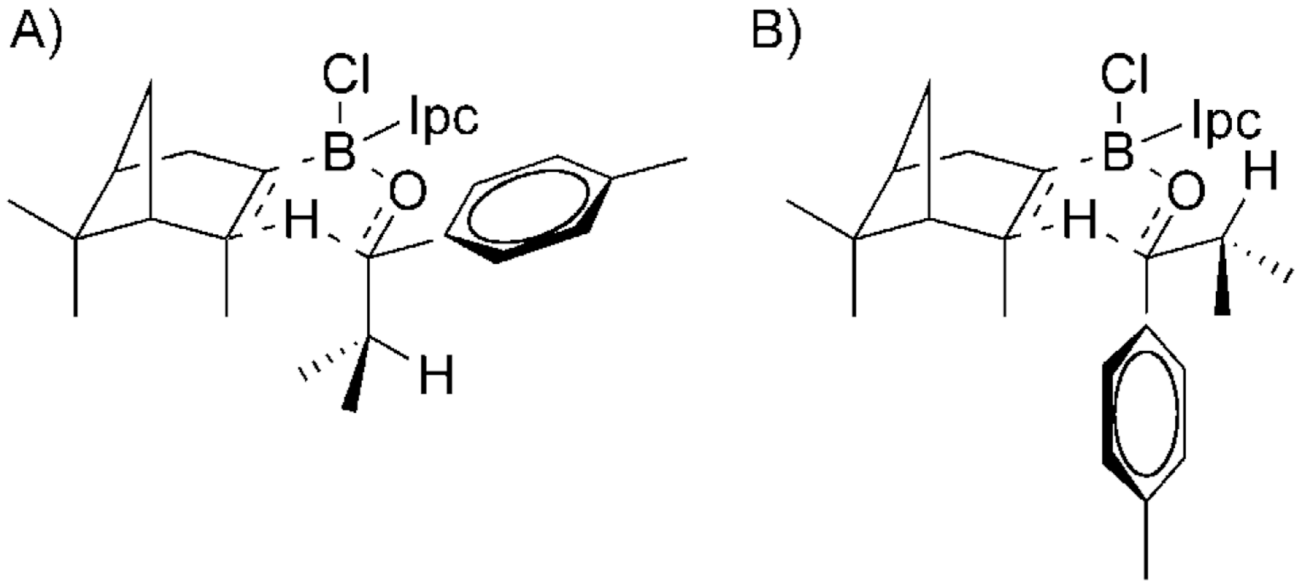

Scheme 4.
Qualitative transition structure models for A) favored *re* attack and B) unfavored *si* attack in the DIP-Cl reduction system.

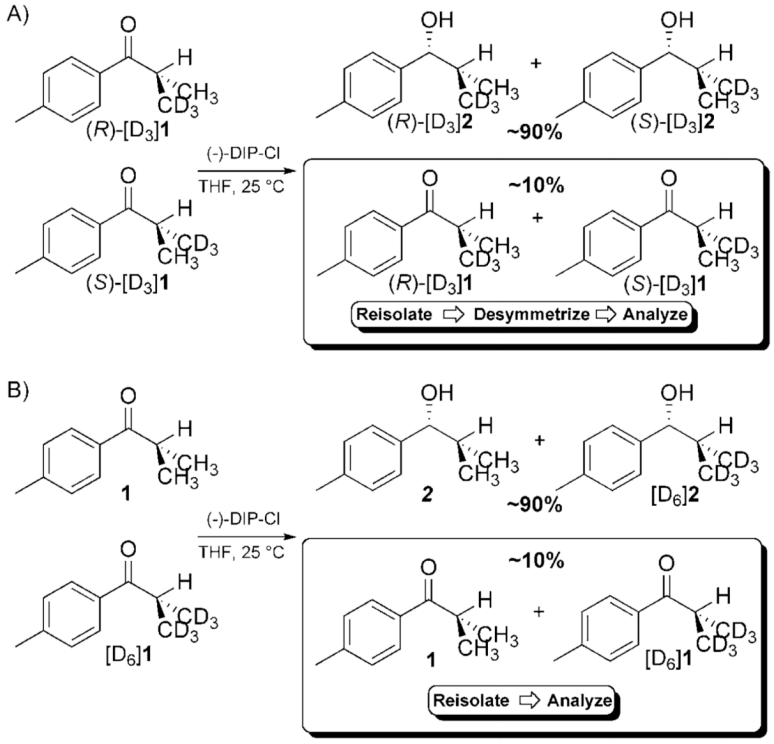

Scheme 5.

The method for measuring ^{2}H KIEs at enantiotopic groups utilizes two competition reactions to yield A) KIE_R and B) KIE_P.

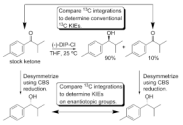

Scheme 6.
Method for measuring ^{13}C KIEs at enantiotopic groups.

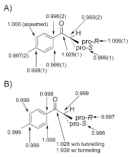

Scheme 7.

A) ^{13}C KIEs measured for the (–)-DIP-Cl reduction of 4′-methylisobutyrophenone. B) ^{13}C KIEs computed by using a transition structure optimized using the B3LYP functional and the 6-31G* basis set.

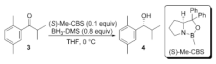

Scheme 8.
The CBS reduction with the variant of the catalyst used here (inset).

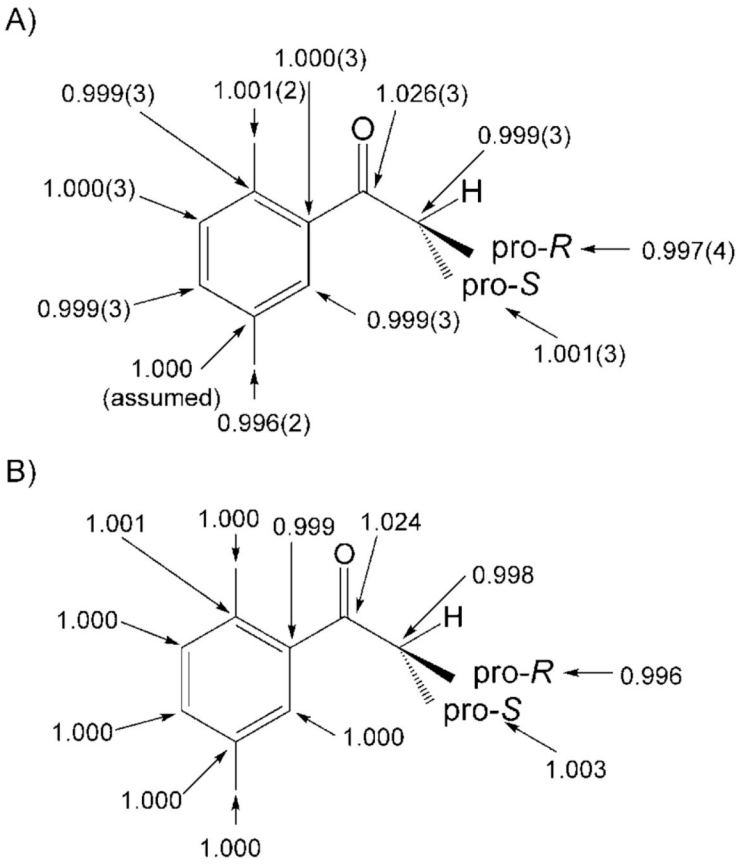

Scheme 9.

A) ^{13}C KIEs measured for the (*S*)-Me-CBS-catalyzed reduction of 2′,5′-dimethylisobutyrophenone. B) ^{13}C KIEs computed by using a transition structure optimized using the B3LYP functional and the 6–31 + G(d,p) basis set.

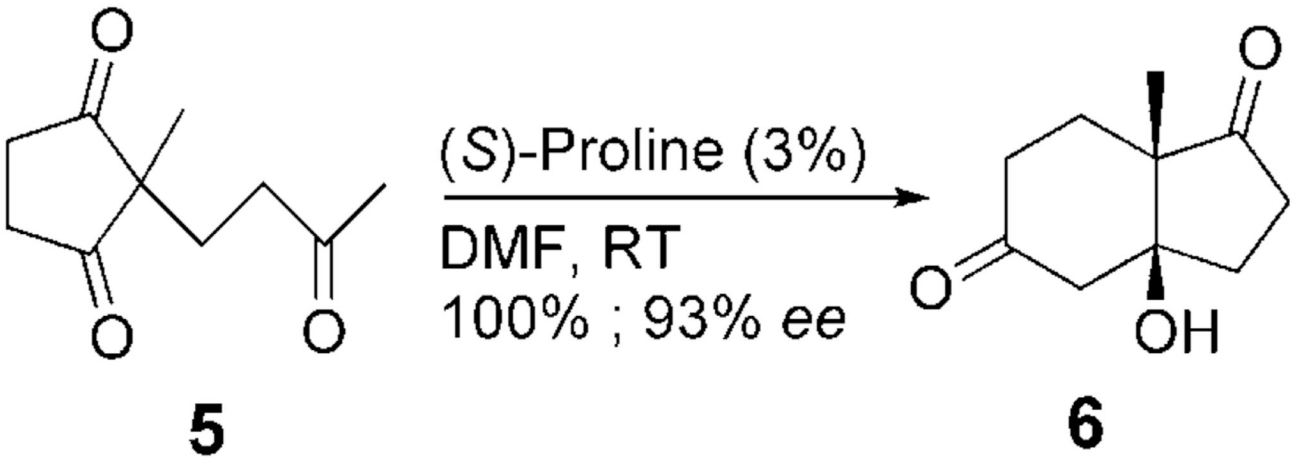

Scheme 10.
Archetypical intramolecular proline-catalyzed aldol reaction.

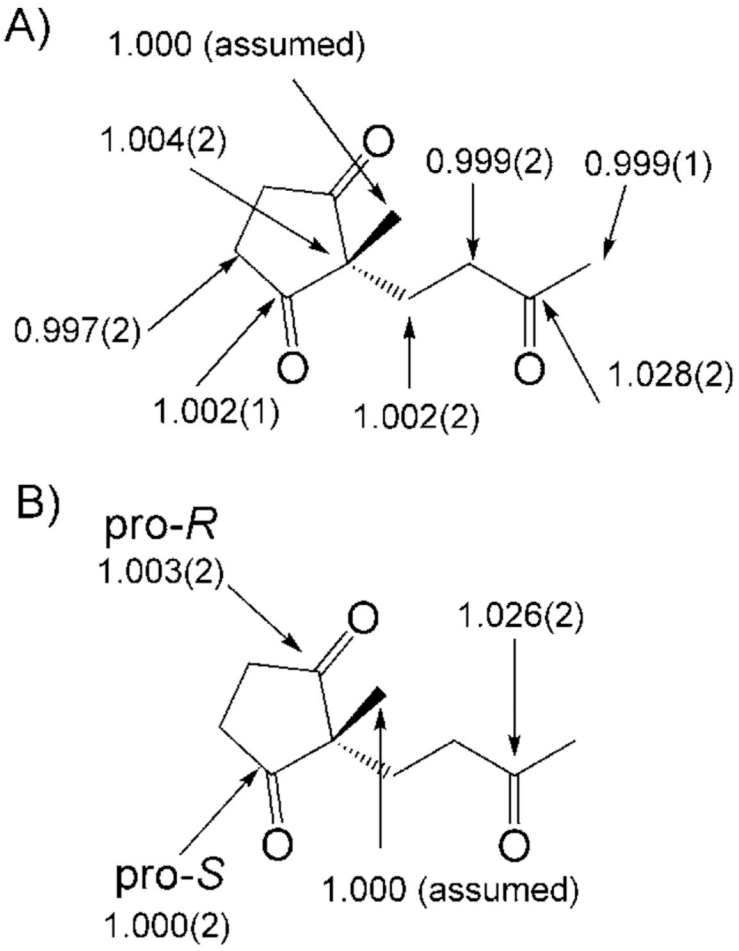

Scheme 11.

Experimentally determined ^{13}C KIEs measured using A) the Singleton method and B) the method presented herein that distinguishes between enantiotopic groups.

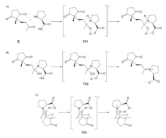

Scheme 12.

Reaction steps and transition-structure models corresponding to A) carbinolamine formation, B) iminium formation, and C) C–C bond formation.

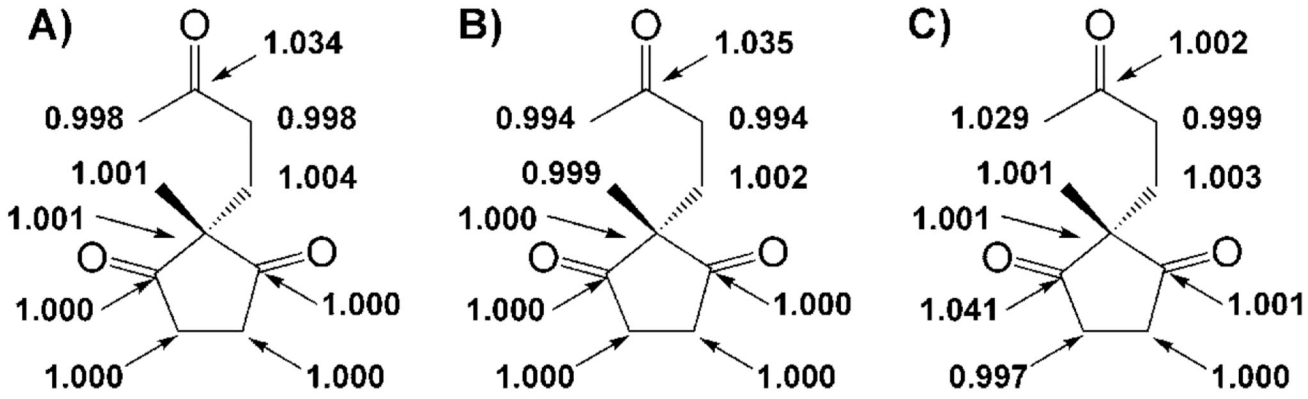

Scheme 13.

Computed ^{13}C KIEs for rate-determining A) carbinolamine formation, B) iminium formation, and C) C–C bond formation. These values were computed from transition structure and reactant models optimized at B3LYP/6–31 + G(d,p) using an IEFPCM model for solvent.